

Multilateral characterization of masks and tubes surfaces in contact with respiratory system through ventilation

A. C. COMAN^a, D. A. TODEA^{a*}, F. POPA^b, T. RADU^c, O. CADAR^d, C. BORZAN^e

^aDepartment of Pneumology, Faculty of Medicine, "Iuliu-Hatieganu" University of Medicine and Pharmacy, 8 Babes Street, Cluj-Napoca, Romania

^bDepartment of Materials Science and Technology, Technical University of Cluj Napoca, 103-105 Muncii Avenue, Cluj-Napoca, Romania

^cFaculty of Physics & Interdisciplinary Research Institute on Bio-Nano-Sciences, "Babes-Bolyai" University, 1 M. Kogalniceanu, Cluj-Napoca, Romania

^dINCDO-INOE 2000, Research Institute for Analytical Instrumentation, 67 Donath Street, Cluj-Napoca, Romania

^eDepartment of Community Medicine, Faculty of Medicine, "Iuliu-Hatieganu" University of Medicine and Pharmacy, 8 Babes Street, Cluj-Napoca, Romania

The aim of this study was to analyse by complementary methods the composition, morphology and real size of inorganic elements, as well as microbiological morphology on the inner surface of continuous positive airway pressure ventilation (CPAP) masks and tubes using scanning electron microscopy (SEM), energy dispersive X-ray spectroscopy (EDX) and X-ray photoelectron spectroscopy (XPS). The images obtained in secondary electrons evidenced a series of homogeneous versus inhomogeneous structures of variable sizes (between 1-200 μm), some of which as separate entities with either rounded or sharp margins, and others grouped in colonies, partly corresponding to a bacterial or fungal variety of microbiological elements. According to elemental distribution maps developed using SEM, it seems that elements (Si, K, P, Ca, Al, Mg, Fe, Ti) form clusters, constituting various metal structures that favours bacterial (main *Staphylococcus*) and fungal adhesion (*Candida*). The presence of microbiological versus inorganic structures on the surface of CPAP masks and tubes raises a flag on the risk of their inhalation into the upper and lower airway. This study allows new researches in the terms of risk factors of home ventilation with CPAP for obstructive sleep apnea syndrome (OSAS).

(Received July 7, 2015; accepted September 9, 2015)

Keywords: Risk, Microbial, Inorganic, Tubes, Masks, CPAP

1. Introduction

The respiratory tract is extremely reactive to the exposure of micron-size inorganic particles, which enter the respiratory tract as aerosols [1]. The concentration of ambient particles depends on their nanometric size and when inhaled, particles in the form of aerosols reach the alveoli, where they deposit, deposition that seems to depend on the rigidity of the alveolar wall [2]. Aerosols deposit in the lungs through several mechanisms: inertial impact, gravitational sedimentation, and diffusion. Small size particles (0.5-5 μm) deposit in the intrathoracic airways by sedimentation that is influenced by gravity [3]. PM10 are indicators for gross particles penetrating into the respiratory tree, while PM2.5 (particles with a nominal mean aerodynamic diameter $\leq 2.5 \mu\text{m}$) were selected to indicate fine particles with a deep penetration in the lungs, in the gas exchange region [4]. If pulmonary defence capacity cannot cope with the invasion of inorganic particles, a local imbalance occurs, which in time generates lung diseases. According to the study of Gradoń et al., it seems however that particle retention and deposition is more accelerated in the pathologically altered lung [2].

Four main groups of chemicals (metallic elements, non-metallic elements, organic compounds and inorganic compounds) contains agents that are known toxins to human beings [5]. Respiratory exposure to silicon (Si) can induce pulmonary fibrosis; prolonged Si exposure causes rigidity of alveolar walls through their infiltration with macrophages and polymorphonuclear neutrophils (PMN) accumulation [6]. Furthermore, respiratory exposure to iron (Fe) can induce siderosis through inhalation of iron oxide metal particles [7]. According to the International Agency for Research on Cancer (IARC), aluminium (Al) could have carcinogenic effects, causing lung cancer and leukemia [8-10]; asthma and chronic obstructive pulmonary disease can also be caused by Al exposure [9]. Magnesium (Mg) exposure can aggravate existing pulmonary disease or, as demonstrated by an experimental study, can generate "metal fever", characterized by fever, cough, dyspnea and leukocytosis [11]. Titanium (Ti) is a mild lung irritant, causing interstitial pneumopathy with cell destruction and mild fibrosis; it can aggravate pre-existing obstructive pulmonary disease [12]. Calcium (Ca) can irritate the eyes, nasal mucosa and skin; it could induce bronchitis and pneumonia. Prolonged Ca exposure could cause dermatitis and nasal ulcerations [13]. Inhalation exposure to phosphorous (P) causes irritation of

the respiratory tract and mucous membranes [14]. Potassium (K) is known to have important effects on the respiratory system when inhaled; even more, when the organism is exposed to high K concentrations, brain oxygen requirements increase [15]. On the other hand, exposure of the respiratory tract to various microbial (bacterial or fungal) species could cause the development of sinusitis, bronchitis or pneumonia, as well as candidosis [16, 17].

Continuous positive airway pressure ventilation (CPAP) used at home for the treatment of obstructive sleep apnea syndrome (OSAS) exposes the airways to the inhalation of fine inorganic particles or various microbial (bacterial or fungal) species, which could cause respiratory diseases. Over the last years, several studies have been published that investigate bacterial contamination of circuits of CPAP or NIV (non-invasive ventilation) therapy at home and their relation with respiratory tract infections [18, 19]. No studies have been published yet to clarify the inorganic, or microbial versus inorganic risk of ventilation devices at home.

The aim of this study was to analyse, by complementary methods, the composition, morphology and real size of inorganic elements, as well as microbiological morphology on the inner surface of CPAP masks and tubing, with which the OSAS patient comes in direct contact during nocturnal CPAP ventilation. Also, for the first time, a modern and innovative surface sampling method, (the double-sided adhesive carbon tape technique) was used. This method allows high performance studies for the characterization of inorganic elements as well as microbial structures.

The investigation methods used in this study (microscopy - SEM, energy dispersive X-ray spectroscopy - EDX and X-ray photoelectron spectroscopy -XPS) offer, for the first time, a complex characterization of the inner surface of masks and tubes used in ventilation. Special attention should be given to the incorporation of antibacterial nanoparticles in the structure of masks and tubes in order to solve the risk of CPAP use for respiratory health. Furthermore, to our knowledge, no studies have been published regarding both inorganic and microbial risk of home CPAP ventilation systems.

2. Experimental

2.1 Sampling

After the informed agreement of the patients was obtained between January and April 2015, samples were collected on a 5 mm x 2.5 mm double-sided adhesive carbon tape with a 5 mm disc diameter, as follows: 44 mask samples and 45 tubing samples from the most exposed and loaded areas of the inner surface of masks and tubing, and 1 mask sample and 1 tubing sample were sterile (for comparison and validation). The masks and tubes used for sampling were provided to patients diagnosed with OSAS in the Sleep Laboratory of "Iuliu Hatieganu" University of Medicine and Pharmacy, Cluj-

Napoca; the patients used nocturnal CPAP ventilation at home, and presented to the Sleep Laboratory for periodic evaluations during the above mentioned period.

The double-sided adhesive carbon tape used in this study has one side that collects the particles to be analysed, while the other side is used to fix the collected sample on a sealed plastic support. The samples were carefully collected by manipulating the double-sided adhesive carbon tape with a tweezer, followed by removing the protective film that cover the side that collects the samples from interest areas.

2.1.1 X-ray photoelectron spectroscopy analysis (XPS)

In order to obtain the elemental composition of the accumulated particles to the carbon tape surface, XPS analysis was used. XP spectra were obtained using monochromated Al K α radiation, operated at 280 W. Spectra were recorded using a SPECS system, with appropriate computer controlled data collection. The base pressure in the spectrometer analysis chamber during experiments was less than 5×10^{-9} mbar. All of the spectra presented in this paper were corrected for the charging effect with reference to the C 1s photoelectron peak at 284.6 eV. Surveys were measured in steps of 1 meV. The data analysis was carried out with the Casa XPS software [20]. The elemental composition on the outermost layer of samples (about 5 nm deep from surface) was estimated from the areas of characteristic photoelectron lines in the survey spectra assuming a Shirley type background.

2.1.2 Scanning electron microscopy (SEM) and energy dispersive X-ray spectroscopy analysis (EDX)

The collected samples were investigated by scanning electron microscopy in order to analyse the fragments accumulated on the carbon tapes regarding morphology, distribution and size. Samples were analysed in a scanning electron microscope (JSM-5600LV, JEOL) equipped with energy dispersive X-ray spectroscopy detector (Oxford Instruments, INCA 200 software). For analysing the chemical elemental distribution of the samples, energy dispersive X-ray spectroscopy analysis was performed. The qualitative analysis of samples was carried out in 5 points for each sample in order to have semi statistical data.

3. Results

3.1. X-ray photoelectron spectroscopy analysis (XPS)

XPS measurements of the samples obtained by exposing the double-sided adhesive carbon tapes to the study areas of interest were performed as described in Section 4.1.1. During its exposure to the established areas,

the tape surface accumulated structures whose elemental composition could be analysed using the XPS method. The spectra obtained by the analysis of the 6 most significant samples, within a wide energy range, 1100-0 eV, are shown in Figure 1a, b, c. XPS spectra are quantified in terms of intensity of the lines (resonance peaks above the baseline) and their position in the spectrum. Peak intensity measures the amount of material found at the surface, while peak position indicates chemical and elemental composition. Thus, based on the analysis of these spectra, the elements present on the sample surface (O, C, Ca, S and Si), as well as their relative concentrations (in atom %) were identified.

Fig. 1a, b, c and Table 1 present the results of XPS in the most representative samples (S03a, S03b, S03c, S03d, S04a, S05a) with the elements present in the obtained XPS spectra and their corresponding concentrations. Data obtained on the carbon tape before its exposure to fragments from the studied environment were also introduced in the table. An increased carbon concentration in the samples was found, possibly due to the fact that the fragments accumulated on the tapes did not completely cover the double-sided adhesive carbon tape, and also, due

to the fact that the surface structure, as evidenced by scanning electron microscopy (next chapter), contained microbiological structures of various types with a carbon in composition; also, O and S may be component elements of microbial protein structures. It is already known that, the standard proteins consist of the following elements: H, C, N, O, S, like those in amino acids L-Cysteine and L-Methionine. The presence of Ca and Si in low concentrations was also identified (Table 1). However, there were no great differences between the samples regarding the concentrations of elements present at the sample surface. This can be explained by the fact that species of the various microbiological structures accumulated on these tapes had similar components. In two of the samples, molybdenum (Mo), derived from the support on which the double-sided adhesive tape was fixed, was detected.

In order to confirm the results of XPS analysis and to evidence the differences occurring in the fragments accumulated on the tapes, particularly regarding their distribution, structure and size, SEM analysis complemented by EDX was performed.

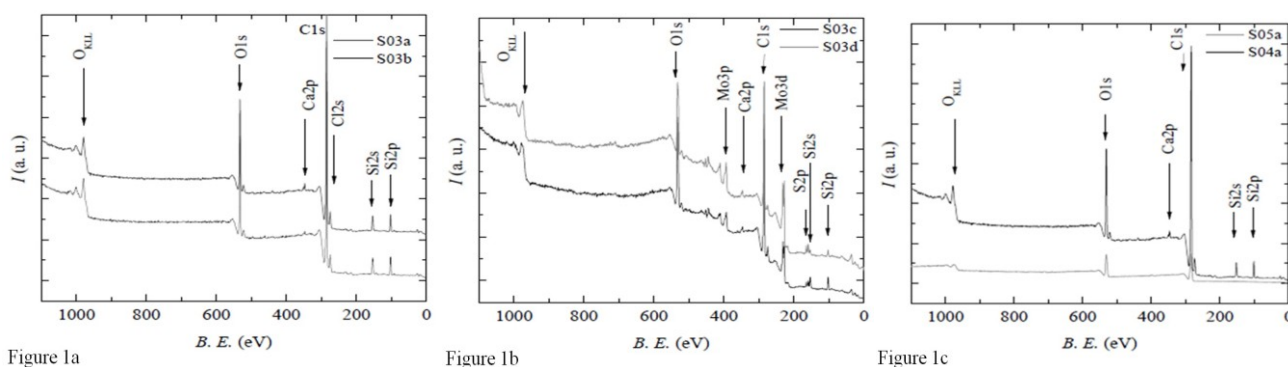


Fig 1. XPS extended spectra obtained from selected samples: a) samples S03a, S03b; b) samples S03c, S03d; c) samples S04a, S05a. Black arrows indicate the identified elements O, Ca, Cl, Si, S, Mo

Table 1. Composition of the surface of samples analysed determined from XPS spectra

Sample	Concentration (at.%)				
	O	C	Ca	Si	S
S03a	18.2	66.5	0.7	5.7	0.8
S03b	14.6	76.4	-	7.7	1.2
S03c	13.7	78.3	0.7	7.2	-
S03d	22.2	50.7	1.3	5	5
04a	20.8	70.5	1.6	7	-
05a	15.8	83.3	0.8	-	-

3.2. Scanning electron microscopy (SEM) and energy dispersive X-ray spectroscopy analysis (EDX)

The images obtained in secondary electrons evidenced a series of homogeneous versus inhomogeneous structures of variable sizes (between 1-200 μm), some of which as separate entities with either rounded or sharp margins, and others grouped in colonies, partly corresponding to a bacterial or fungal variety of microbiological elements. In order to evidence the species present in the collected samples, a large-scale analysis (low magnification – 100x – evidencing large structures) and a small-scale analysis (magnifications in the order of 10000-20000x – evidencing bacterial and fungal structures) were used.

A magnification of 10000x evidences small structures which can pose a risk for respiratory health as a result of their long-term inhalation or direct contact with anatomical structures, because they have varied shapes, including irregular sharp or edgy margins.

In order to determine the nature of the observed structures, elemental distribution maps of the analysed areas were created. Thus, it was attempted to combine visual information and chemical analysis for identifying and discussing the possible microbiological type, with the

mention that the entire studied sample group was quasi-identical in structure and appearance.

Figure 2a (200x) evidences a cluster of skeletal tubular structures composed of C, O, Cl, Na, Si, P and S according to EDX, not presented here, which occur on a background shown in Figure 2b (500x), smooth, slightly bosselated, with round agglutinations of quasi-identical shapes, similar to staphylococcal colonies; there are also other examined materials with a similar distribution. The chemical elements detected in the tubular structures have a biological origin.

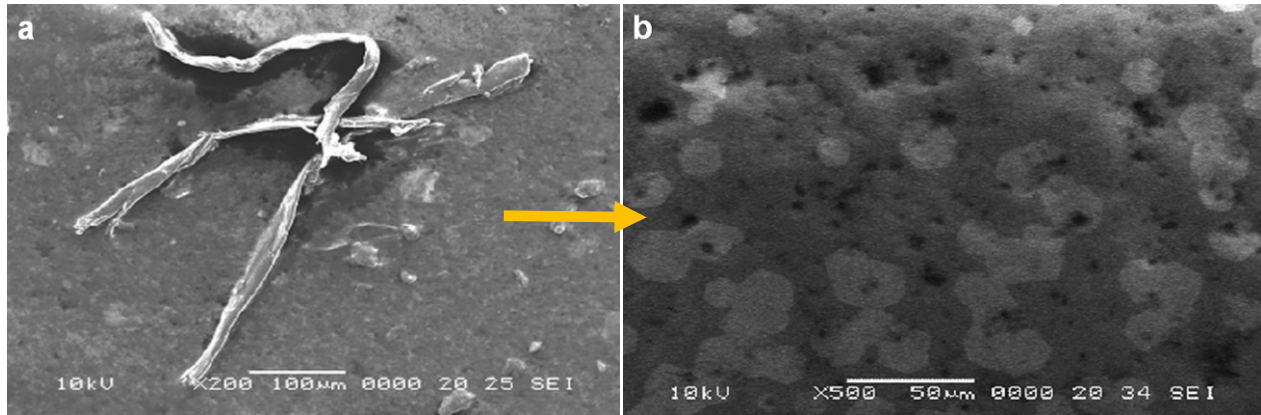


Fig. 2. Electron microscopy micrographs of S05a sample collected from the mask: (a) skeletal structures at 200 x magnification and (b) bacterial adhesion at 500 x magnification on carbon tape

In Fig. 3 there are large amounts of Na and Cl as well as O, C, Si and S, suggesting a physiological saline structure eliminated during respiration; the background

consists in very high numbers of colony-like clusters similar to the *Staphylococcus* type [21].

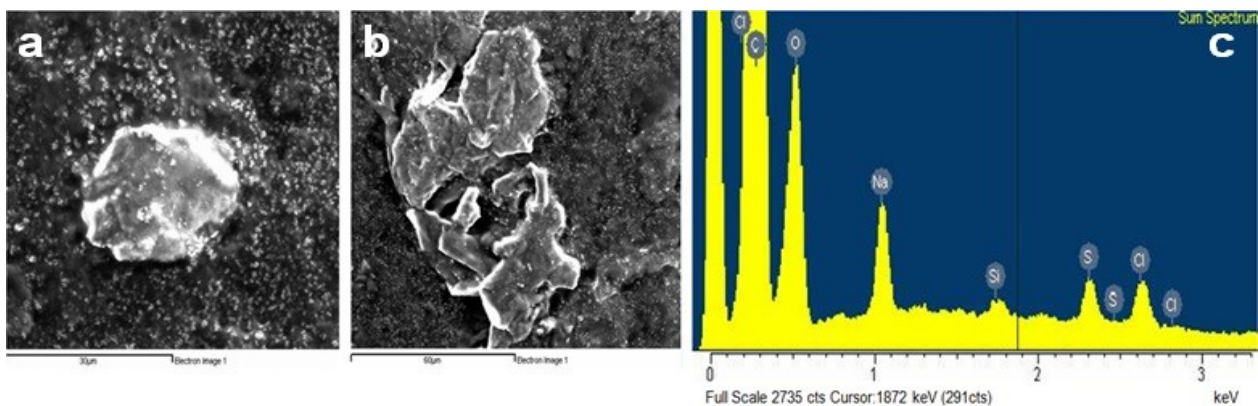


Fig. 3. Characterisation of the sample S05a collected from the mask (a and b) SEM micrograph of sample at different magnification; (c) EDX spectrum of the sample

Fig. 4 shows, in the background, many smooth structures with sharp edges, <math><10\ \mu\text{m}</math> in size, with chemical elements such as C, O, Al, Ti, Si, K. Due to their shape and small size, these structures can pose a risk through

direct contact with the upper and lower airways, depending on the surface where they are located.(e.g. mechanical lesions of the soft tissues).

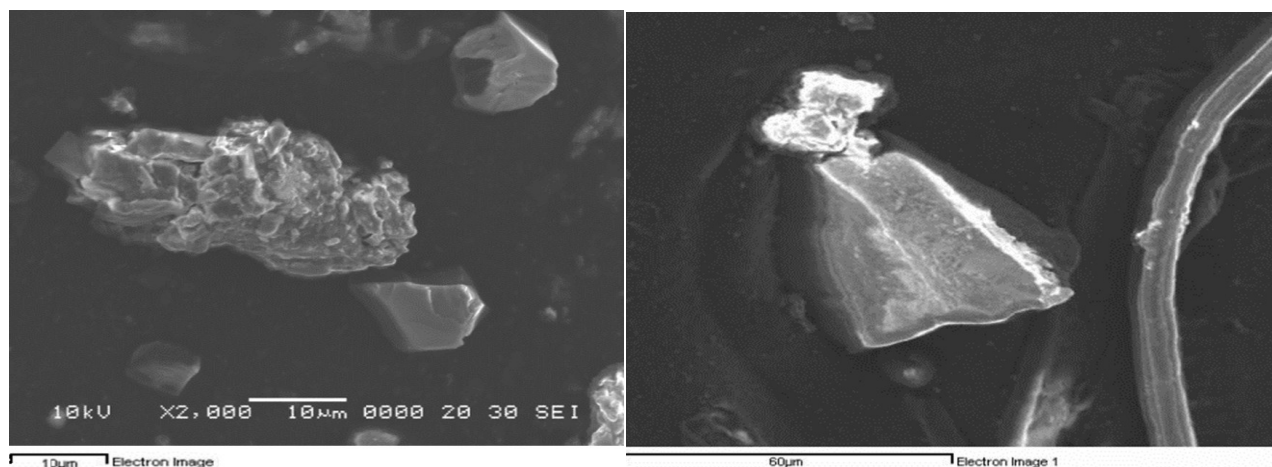


Fig. 4. Electron microscopy micrographs of S017b sample collected from the tubing. SEM images show the presence of structures on the carbon tape with different shapes and sizes (scale bar from 10-60 μm)

Fig. 5 evidences a structure about 30 μm in diameter, containing in composition the following elements: C, O, Al, Ti, Si, K according to EDX analysis. On such structures small colony-like structures similar to

Staphylococcus colonies are visible to adhere, as pointed in the Fig. 5a [21]. Practically, bacterial colonies adhere to metal elements.

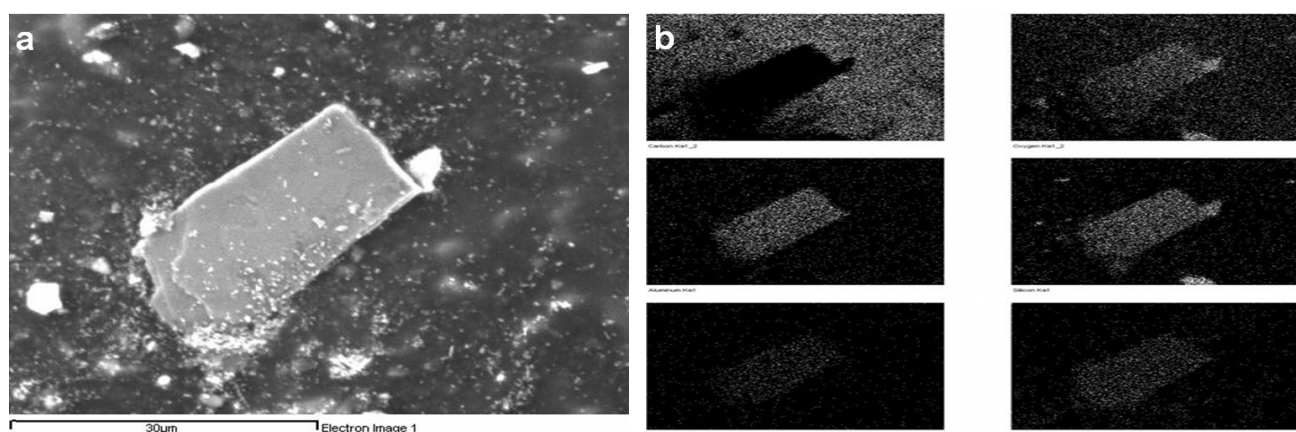


Fig. 5. Characterisation analysis of the sample S017b collected from the tubing (a) SEM micrograph of sample; (b) EDX spectrum of the sample

Fig. 6 (a and b) shows microbial agglutinations similar to *Staphylococcus* on surfaces containing metal structures such as Ti, Fe associated with C, O, S, Ca according to EDX analysis. The same bacterial *Staphylococcus aureus*-like cluster occurs in Figure 6 c, with an EDX spectrum identifying C, O, Al, Na, Si, S, Cl,

Ca. *Staphylococcus aureus*-like colonies are small, round, adherent to the surface. This description provides additional elements that reinforce the idea according to which metal elements described on the surface of CPAP masks favorise microbial colonization.

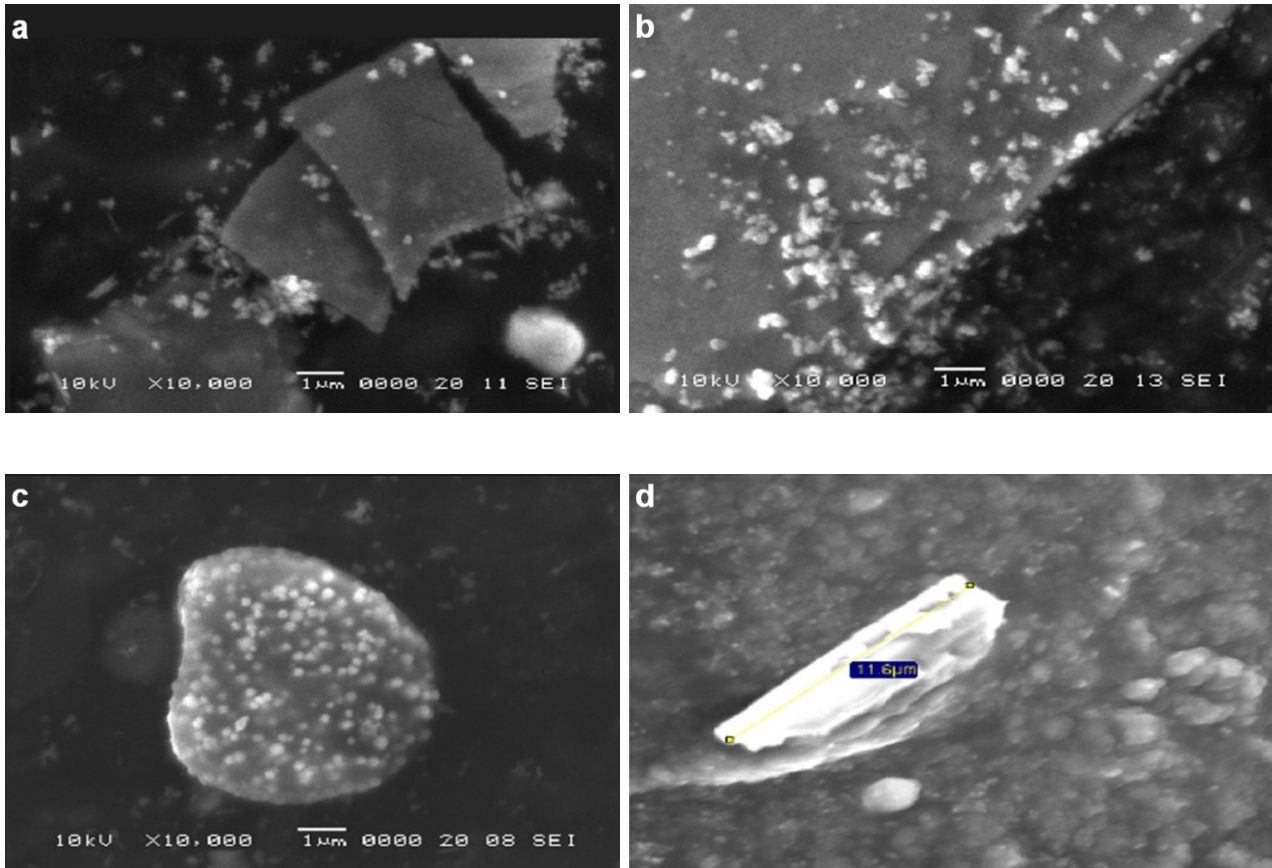


Fig.6. Electron microscopy of the sample S017a collected from the mask reveals *Staphylococcus* colonies on surfaces containing metal structures (a),(b) – variable shapes and sizes of bacterial colonies adherent to surfaces, (c) – similar shapes and sizes of bacterial colonie adherent to surface, (d) – skeletal 11.6 μm structure (scale bar 1 μm)

On the background of the previously described microbiological entities, a 11.6 μm element with bosselated, slightly sharp margins, which seems to be a disintegrated structure, is evidenced (Figure 6d).

Fig. 7 (a and b) corresponds to residual bacterial, possibly also fungal and *Candida* structures [22], while

Fig. 7c is similar, in appearance, to *Staphylococcus* colonies. Shapes are variable and sizes are small, ranging from 10 μm to < 1 μm . Figure 7d shows colonies possibly of a different type of *Candida* from that of Figure 7b.

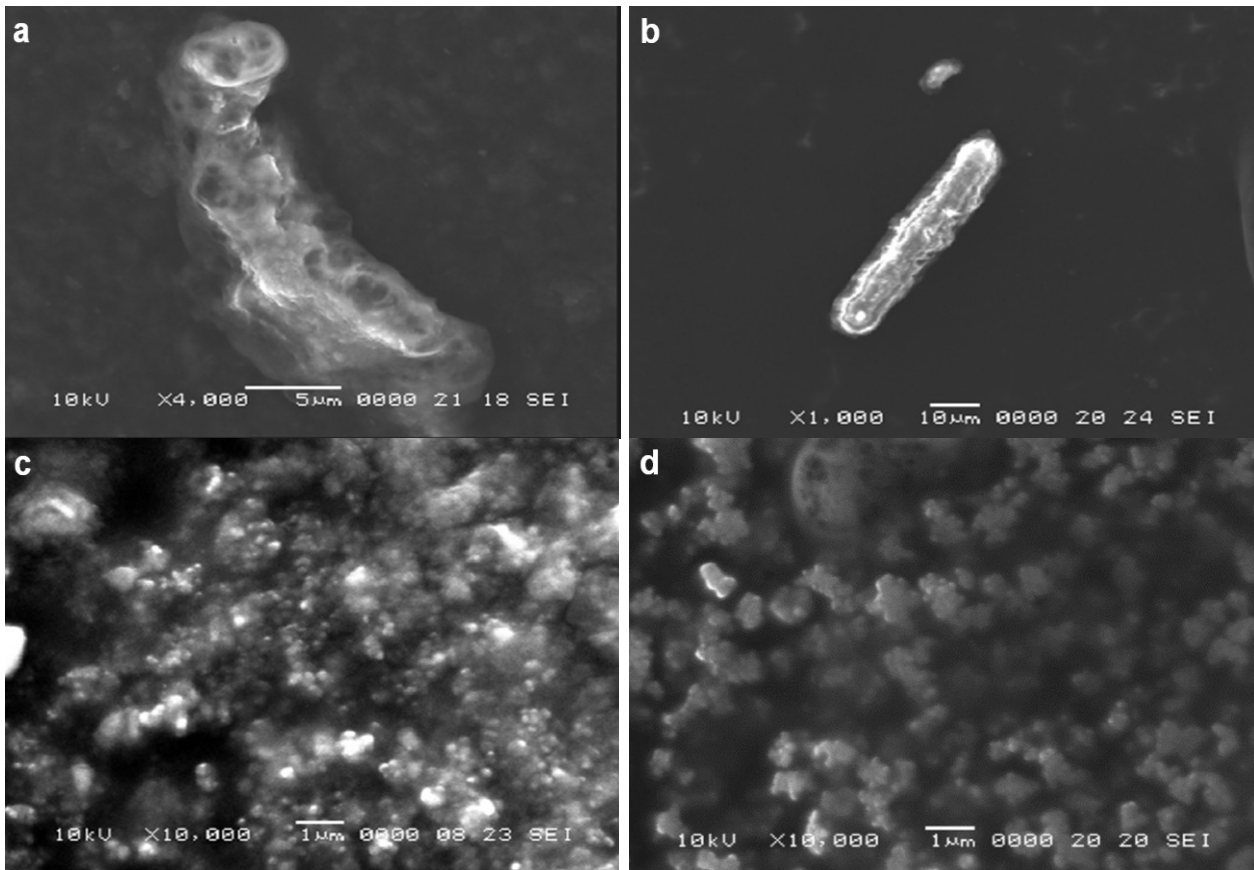


Fig.7. SEM micrographs of S024a sample collected from the mask; (a) single residual structure (b) – single well delimited structure (c) – multiple similar shapes and sizes of bacterial colonies (d) – multiple similar shapes and sizes of fungal colonies (scale bar from 1-10 μm)

4. Discussion

According to elemental distribution maps developed using SEM, it seems that elements (Si, K, P, Ca, Al, Mg, Fe, Ti) form clusters, constituting various metal structures that favour bacterial adhesion. Thus, it can be concluded that microbial structures can fix to inorganic structures present on the samples, posing a double risk of exposing the upper and lower airways to fine metal particles and various microbial colonies. Similar results were obtained by Eqawa et al. [23] and by Shida et al. [24] regarding the capacity of adhesion of *Staphylococcus epidermidis* to prosthetic biomaterials; bacterial adhesion to Zn and Ti surfaces has important applicability to Ti implants in oral medicine. Over the last years, many studies were focused on bacterial adhesion on surfaces in urinary, cardiac, bone or skin area [25], but no studies were designed in the respiratory field. However, the mechanisms of bacterial adhesion to biomaterials are very complicated and not yet fully understood. [25] There are no data in the literature to compare with, regarding the bacterial adhesion to metal surfaces (Al, Mg, Fe, Ti) during ventilation with CPAP devices.

The most frequent microorganisms evidenced in our study seem to be *Staphylococcal* colonies of various types and *Candida* colonies. Other microorganisms could be present but on the analysed samples they were not found.

Similar results were published by Rodríguez González-Moro et al. [18] which investigate the prevalence of bacterial contamination of ventilators using NIV at home; according to the results the most frequently encountered microorganism was *Staphylococcus aureus*. Respiratory exposure to these microorganisms can induce upper and lower respiratory infections [16, 17]. According to Sanner et al. upper respiratory infections were more frequent in patients who use CPAP than in control patients (13.6% vs 2.5%) [19]. Indeed, a limitation of our research is the absence of data on the potential airway infections of the patients.

Our study identifies many colonies consistent with fungal species. There are no specific literature data regarding the use of CPAP devices and development of respiratory fungal diseases. There are some studies regarding mechanical ventilation and development of fungal diseases, but in intensive care units. Azoulay et al. [26] were among the first who hypothesize the presence of *Candida* spp. in the airways of mechanically-ventilated patients. Furthermore, many studies demonstrate the association of mechanical ventilation and presence of *Candida* [27-29].

Simu et al., illustrates the usefulness of SEM, EDX and XPS in the complex characterization of aerosols from dental offices as risk factors for health, and demonstrates that aerosols derived from various dental procedures are

extremely diverse and can penetrate into the respiratory tree up to the alveoli, causing serious adverse effects on the health of doctors and patients [30]. Our study identifies with the similar techniques some of the chemical elements evidenced in the study mentioned above, which are in smaller amounts; additionally, it identifies many bacterial and fungal structures that can be derived from the oronasal region [16] as well as from the non-replacement of CPAP machine accessories according to norms [31], or to their defective hygiene. The higher number of identified bacterial family is probably related with the more “fluid contact” of the procedure compared with the air transferred bacteria in our case.

A recent study performed by Brown et al. [1] estimates the mean size of deposition of particles in the respiratory tract of adults compared to children at $\sim 5 \mu\text{m}$ for children and $\sim 3 \mu\text{m}$ for adults. These estimates of particle penetration, slightly different from PM10 theories, could be useful in the future in designing experimental studies for the interpretation of PM sizes with effects on respiratory tract health. All patients included in our study were adults exposed to various chemical elements and biological structures with variable diameter from $\sim 1 \mu\text{m}$, some of which ranged in classes of risk for the respiratory system.

Starting from these aspects, it would be interesting to study in the future the possibilities to incorporate nanoparticles that are currently known to have antimicrobial effects in the structure of masks and tubing; this would allow to reduce microbial load, as well as to prolong the duration of use of a mask. The applicability of nanoparticle synthesis has extensively developed in medicine, particularly with the occurrence of antibiotic resistant bacterial species [32]. There is a current interest in finding solutions to reduce health risks by innovative methods in all fields; for example, in dental medicine, a biocompatible material has been recently synthesized which can be used to diminish oral health risk [33].

This study provides important elements for extending the application of nanotechnology in respiratory and sleep medicine, field of scientific and medical interest that has not been researched so far, to our knowledge.

5. Conclusions

This study demonstrates, for the first time, the presence of various microbiological and inorganic structures on the inner surface of CPAP masks and tubes, with the possibility to specifically detail their exact shapes and sizes. This specific characterization emphasize the risk of microbial and inorganic elements inhalation into the upper and lower airways on the one hand, and the safety measures that need to be implemented in order to reduce this risk, on the other hand. The development of bio nanotechnology highlights clear evidence entailing the imminent application of hygiene measures in this type of therapy both locally and in the structure of the materials used, while it also provides solutions in this regard. Future studies on the synthesis of nanoparticles that can be

incorporated in the structure of masks could solve the risk of CPAP use for respiratory health.

Furthermore, this study represents a start for new researches in the terms of how home ventilation with CPAP for OSAS can expose respiratory tract to risk factors such as microbiological structures and inorganic elements.

Acknowledgements

This paper was co-financed and published under the frame of the European Social Fund through the Sectoral Operational Programme Human Resources Development 2007-2013, project number POSDRU/107/1.5/S/ 82705.

References

- [1] J. S. Brown, T. Gordon, O. Price, B. Asgharian, *Part Fibre Toxicol* **10**, 12 (2013).
- [2] L. Gradoń, D. Orlicki, A. Podgórski, *Int J Occup Saf Ergon* **6**, 189 (2000).
- [3] C. Darquenne, *J Aerosol Med Pulm Drug Deliv* **27**, 170 (2014).
- [4] U.S. Environmental Protection Agency (U.S. EPA), National ambient air quality standards for particulate matter; final rule, *Fed Regist* **62**, 38652 (1997).
- [5] W. J. Rea, K. D. Patel, *Volume 2: The Effects of Environmental Pollutants on the Organ System*, CRC Press: Taylor and Francis Group, Boca Raton, USA (2014).
- [6] www.cdc.gov/niosh/docs/81-123/pdfs/0552.pdf, Occupational Health Guideline for Amorphous Silica, available online June (2015).
- [7] <https://cdn.intechopen.com/pdfs-wm/27232.pdf>, available online June (2015).
- [8] F. Van Schooten, F. Jongeneelen, M. Hillebrand F. E. van Leeuwen, A. J. van Looff, A. P. Dijkmans, J. G. van Rooij, L. den Engelse, E. Kriek, *Cancer Epidemiol Bio Prev* **4**, 69 (1995).
- [9] C. Tremblay, B. Armstrong, G. Thériault, J. Brodeur, *Am J Ind Med* **27**, 335 (1995).
- [10] D. Hendrick, P. S. Burge, W. Beckett, A. Churg, *Occupational disorders of the lung*, London, WB Saunders, Harcourt pp. **201-219** (2002).
- [11] www.cdc.gov/niosh/docs/81-123/pdfs/0374.pdf, Occupational Health Guideline for Magnesium Oxide Fume, available online June (2015).
- [12] www.cdc.gov/niosh/docs/81-123/pdfs/0617.pdf, Occupational Health Guideline for Titanium Dioxide, available online June (2015).
- [13] www.cdc.gov/niosh/docs/81-123/pdfs/0093.pdf, Occupational Health Guideline for Calcium Oxide, available online June (2015).
- [14] https://archpdfs.lps.org/Chemicals/Phosphorus_white.pdf, available online June (2015).
- [15] L. Hertz, T. Clausen, *Biochem J* **89**, 526 (1963).
- [16] I. S. Gomes-Filho, J. S. Passos, S. Seixas da Cruz, *J Oral Microbiology* **2**, 10.3402 (2010).

- [17] <http://wwwnc.cdc.gov/travel/yellowbook/2014/chapter-2-the-pre-travel-consultation/respiratory-infections>, available online June (2015).
- [18] J. M. Rodríguez González-Moro, G. Andrade Vivero, J. de Miguel Díez, S. López Martín, C. Sánchez, J.L. Izquierdo Alonso, P. de Lucas Ramos, *Arch Bronconeumol* **40**, 392 (2004).
- [19] B.M. Sanner, N. Fluerebrock, A. Kleiber-Imbeck, J.B. Mueller, W. Sidec. *Respiration* **68**, 483 (2001).
- [20] N. Fairley, A. Carrick, *The Casa Cookbook—Part I: Recipes for XPS Data Processing* (Acolyte Science, Knutsford, Cheshire, England (2005).
- [21] A. Kazunobu, A. Umeda, *Journal Ultra Res* **58**, 1, 34 (1977).
- [22] D. R. Radford, S. J. Challacombe, J. D. Walter, *J. Med. Microbiol* **40**, 416 (1994).
- [23] M. Egawa, T. Miura, T. Kato, A. Saito, M. Yoshinari M., *Dent Mater J* **32**, 101 (2013).
- [24] T. Shida, H. Koseki, I. Yoda, H. Horiuchi, H. Sakoda, M. Osaki, *Int J Nanomedicine* **8**, 3955 (2013).
- [25] M.Katsikogianni, Y.F.Missirlis, *European Cells and Materials*. Vol.8, pages 37-37 (2004).
- [26] Azoulay E, Timsit JF, Tafflet M, de Lassence A, Darmon M, Zahar JR, Adrie C, Garrouste-Orgeas M, [Cohen Y, Mourvillier B, Schlemmer B *Chest* **129**,110 (2006).
- [27] J.D.Ricard, D.Roux, *Intensive Care Med* **38**, 1243 (2012).
- [28] A. Y. Peleg, D.A. Hogan, E.Mylonakis, *Nat Rev Microbiol* **8**, 340 (2010).
- [29] D. Roux, S. Gaudry, D. Dreyfuss, ElBenna, de Prost N, E. Denamur, G. Saumon, J.D.Ricard, *Crit Care Med* **37**:1062–1067(2009).
- [30] M. R. Simu, C. Borzan, M. Mesaros, M. T. Chiriac, T. Radu, *Dig J Nanomater Bios* **9**, 1429 (2014).
- [31] D. R. Levinson, *Replacement Schedules for Medicare Continuous Positive Airway Pressure Supplies*, (OEI-07-12-00250) June (2013).
- [32] J. T. Seil, T. J. Webster, *Int J Nanomedicine* **7**, 2767 (2012).
- [33] M. R. Simu, R. Ciceo-Lucacel, O. Ponta, C. Borzan, M. Mesaros, T. Radu, *Dig J Nanomater Bios* **9**, 1529 (2014).

*Corresponding author: doina_adina@yahoo.com